Hybrid Solid Polymer Electrolytes Based on Epoxy Resins, Ionic Liquid and Ceramic Nanoparticles for Structural Applications

Bianca K. Muñoz *, Jorge Lozano Martín, Maria Sanchez, Alejandro Ureña

Posted Date: 26 June 2024

doi: 10.20944/preprints202406.1894.v1

Keywords: Solid Polymer Electrolyte; Composite Polymer Electrolyte; Structural supercapacitor; Energy storage; Structural devices

 doi:10.20944/preprints202406.1894.v1

Article

Hybrid solid polymer electrolytes based on epoxy resins, ionic liquid and ceramic nanoparticles for structural applications

Bianca K. Muñoz *, Jorge Lozano, María Sánchez and Alejandro Ureña

Material Science and Engineering Area, Universidad Rey Juan Carlos, ESCET, C/Tulipán s/n. Móstoles, 28933 Madrid, Spain

* Correspondence: bianca.munoz@urjc.es. Tel.: +34-91-488-71-45

Abstract: Solid polymer electrolytes and composite polymer electrolytes serve as crucial components in all-solid-state energy storage devices. Structural batteries and supercapacitors present a promising alternative for electric vehicles, integrating structural functionality with energy storage capability. However, despite their potential, these applications are hampered by various challenges, particularly in the realm of developing new solid polymer electrolytes that require more investigations. In this study, novel solid polymer electrolytes and composite polymer electrolytes were synthesized using epoxy resin blends, ionic liquid, lithium salt, and alumina nanoparticles, and subsequently characterized. Among the formulations tested, the optimal system, designated as L70P30ILE40Li1MAl2 and containing 40 wt.% of ionic liquid and 5.7 wt.% of lithium salt, exhibited exceptional mechanical properties. It displayed a remarkable storage modulus of 1.2 GPa and reached ionic conductivities of 0.085 mS/cm at 60°C. Furthermore, a proof-of-concept supercapacitor was fabricated, demonstrating the practical application of the developed electrolyte system.

Keywords: solid polymer electrolyte; composite polymer electrolyte; structural supercapacitor; energy storage; structural devices

1. Introduction

Multifunctional structural supercapacitors and batteries are considered an outstanding approach for energy storage in electrical vehicles (EVs). It is well-known that reducing weight in a vehicle can help to reduce the fuel consumption. This statement has also been estimated in terms of energy consumption (around 7%) when weight is reduced in 10% [1,2]. Based on this fact, the electrical vehicles have different forms of reducing weight, the most intuitive consist in using lightweight materials (fiber composites or aluminum matrix composites), a well-stablished path [3]. Another potential way includes using structural materials as energy storage devices themselves, the most attractive route but still far from practical implementation and commercialization [2,3]. The synergic combination of lightweight resistant materials as carbon fiber reinforced polymers (CFRP) with their ability for energy storage (supercapacitors, batteries and fuel cells) and detaching the inert battery mass (needed but useless), appears as an ideal scenario for achieving a practical fuel independency [4]. From the components of the multifunctional devices the recent studies have been address to the modification of carbon fiber electrodes, development of solid polymer electrolytes, glass or Kevlar fiber separators, current collector, etc.

The solid polymer electrolyte (SPE) are key components of the structural supercapacitors and batteries, and they are still at their early stage of development since their ionic conductivities are not comparable to liquid electrolytes and are far from 1 $mS \cdot cm^{-1}$ at low temperatures. In this context, different approaches have been done so far with various degrees of success and some technical issues, as the stability window and ionic conductivity, that are not high enough to appear as a competitive option. Hybrid Electrolytes (HE) or Composite Polymer Electrolytes (CPE) are electrolytes with more

 doi:10.20944/preprints202406.1894.v1

than two components that can be an alternative to traditional electrolytes to simultaneously improve ionic conductivity and mechanical properties. They have been classified as active and passive electrolytes, depending on the nature of their reinforcements and whether they participate or not in the conduction mechanism. Electrolytes with ceramic reinforcements that do not provide ionic movement by themselves, such as SiO_2 or TiO_2, are considered passive. Passive HE has recently attract the attention of researchers because they exhibit higher mechanical resistance and thermal stability than active HE, being less expensive and more accessible [5–9]. For instance, alumina has been reported to modify the ionic conductivity in polymer electrolytes by preventing the formation of crystals and improve the mechanical properties due to their rigid nature [10–13]. Some examples of its used have been reported in poly(vinyl alcohol) (PVA) matrices, where it has been observed that using nano-alumina in 6 wt% showed a remarkable increase in conductivity due to the increase of amorphous areas in PVA. Above 6 wt% aggregation of alumina NPs that creates unsuitable paths for ion transfer has been detected [10]. Also, many studies have used alumina as reinforcement in a poly(ethylene oxide) (PEO) matrix including a lithium salt [14,15].

Epoxy resins are appropriated matrices for structural applications [16]. Those derived from Polyethylene Glycol Diglycidyl Ether (PEGDGE) or diglycidyl ether of bisphenol A (DGEBA) has been investigated as SPEs [17–21]. Kwon *et al.* reported the introduction of alumina nanowires (2-6 nm) in epoxy resin/Li salt system. They have observed that an increase in the amount of alumina has increased the conductivity (0.29 $mS{\cdot}cm^{-1}$ at 25 °C), and certain content result in reducing the ion dissociation due the NPs aggregation. Also, it has been observed that alumina can act as a plasticizer decreasing the T_g of the polymer [12]. Another successful example has been reported by Choi and coworkers, where the solid polymer electrolyte based on DGEBA, succinonitrile and lithium salt afford ionic conductivities from 1×10^{-3} to 0.1 mS/cm, reaching a high Young's modulus of 1 GPa in some cases [22].

Recently in our group, we have developed HEs based on a mixture of epoxy resins with PEGDGE, and a commercial epoxy resin (Araldite LY556) based on diglycidyl ether of bisphenol A (DGEBA), using a commercial hardener Araldite XB3473 and 4,4-diphenylsulfone. The additives used were ionic liquid and titania nanoparticles. These electrolytes showed good mechanical properties (T_g > 70°C and storage modulus at 30°C > 1 GPa) and promising ionic conductivities [18]. Using the same epoxy resin system a systematic study was done including different alumina content (2-8 wt.%) [23]. In this study the best system found (2 wt. % Al_2O_3) was able to afford outstanding mechanical and thermomechanical performance (Tg = 83 °C and E′ at 30 °C = 1.2 GPa) and moderate ionic conductivities at RT ($\sigma_1 = 1.6 \times 10^{-3}$ mS/cm). This family of electrolytes was found to be very appropriate for structural applications, as it has been demonstrated in the fabrication of a structural supercapacitor, which exhibit a Young Modulus of 24.0 ± 1.6 GPa and a tensile strength 294 ± 9 MPa [24]. From a mechanical point of view the CFRP obtained with this electrolyte formulation achieve an ideal behavior for energy storage devices, since in some practical examples for batteries the Young Modulus and tensile strength reported are in the range of 1.8-25 GPa and 90-300 MPa, respectively [25].

Here we report new solid polymer electrolyte and composite polymer electrolytes for structural lithium batteries. The new lithium SPEs and CPEs are based on epoxy resin blends, ionic liquid, lithium salts and alumina nanoparticles. The best formulation found achieves a storage modulus 1,2 GPa and T_g of 73ºC with an ionic conductivity of 1.8×10^{-3} mS/cm by introducing less than 10 wt.% of lithium salt. This electrolyte represents a promising alternative in the development of more efficient and safer structural batteries.

 doi:10.20944/preprints202406.1894.v1

2. Materials and Methods

2.1. Materials

Solvents and reagents were purchased and used without further purifications. Epoxy resins Araldite LY556 based on Diglycidyl Ether of Bisphenol A and its crossing agent XB3473, were provide by Huntsman. The epoxy resin has an epoxy equivalent mass range of 183.48-188.67 epoxy equiv^{-1}. The amines equivalent mass range of the crossing agent wa 82.6-89.3 g amine equiv^{-1}. The ratio Epoxy resin/hardener used was 100:23 wt.%, according to the supplier recommendations and this system was identified as **L**. The reagents Poly(ethylenegycol) Diglycidyl Ether (PEGDGE, Mn 500), diaminodiphenylsulfone (DDS), and the lithium salt bis(trifluoromethylsulfonyl)imide lithium (LiTFSI, **Li**) and alumina nanoparticles (**Al**, 13 nm) were purchased in Merck. Ionic liquid 1-ethyl-3-methyl-imidazolium bis(trifluoromethylsulfonyl) imide (**ILE**, 99%) was acquired in IOLITEC. The resin system PEGDGE/DDS used an epoxy/amine ratio of 100:35 wt.% and it was identified as **P**.

The nomenclature used for the reagents and epoxy resins are mentioned or appear in parentheses in bold capital letters as shown above.

2.2. Methods

All the samples were characterized by Dynamic Mechanical Thermal Analysis (DMTA), Cyclic Voltammetry (CV), Linear Sweep Voltammetry (LSV), Electrochemical Impedance Spectroscopy (EIS) and Field-Emission Gun Scanning Electron Microscopy (FEGSEM).

2.2.1. Dynamic Mechanical Thermal Analysis (DMTA)

The thermo-mechanical properties were studied following the ASTM 5418 in a DMTA Q800 V7.1 (TA Instruments) in a single cantilever mode over a temperature range from 25-275 °C, using a ramp of 2°C/min and a frequency of 1 Hz. The thermal scanning was done from -50 to 200 °C, to determine the glass transition temperature (T_g), which was measured as the maximum of the loss tangent curve (tan δ). In addition, the average modulus at room temperature allows evaluating the stiffness of the samples.

2.2.2. Cyclic Voltammetry (CV) and Linear Sweep Voltammetry (LSV)

The CV y LSV analysis were done to determine the stability window and electrochemical behavior of the electrolytes. The measurements were done in a potentiostat AUTOLAB PGSTAT302N with a software Nova 2.1. The CV parameters were from -1 to 1 V at 10 mVs^{-1} and for LSV the potential varied from 0 to 4 at the same scan rate.

2.2.3. Electrochemical Impedance Spectroscopy (EIS)

The samples for EIS were dried in an oven at 80°C during overnight after being painted with silver ink to favor the electrode-electrolyte contact. The EIS analysis was done in a potentiostat AUTOLAB PGSTAT302N. The samples were sandwiched between two symmetric clean and polished stainless-steel electrodes and introduced in a homemade press hold sampler to improve the electrolyte-electrode contact. The impedance of the samples was measured at room temperature using a frequency range between 1.0 MHz and 0.1 Hz and an amplitude of 30 mV. The Nyquist Plots (Imaginary contribution of impedance Z″ vs Real contribution Z′) showed a semicircle at high frequencies and an additional contribution at lower frequencies corresponding to R_0(CPE_1 R_1) (CPE_2 R_2) equivalent circuit. The ionic conductivities were obtained from R_1 for the solid polymer electrolytes following Equation (1). The composite polymer electrolytes (those containing alumina nanoparticles) showed two conduction paths due to the reinforcement and two ionic conductivities were obtained from R_0 and R_1, respectively.

$$\sigma = \frac{d\ (cm)}{R\ (\Omega) \times A(cm^2)} \quad (1)$$

 doi:10.20944/preprints202406.1894.v1

2.2.4. Chronoamperometry for lithium transference number calculations (t_{Li^+})

The samples were sanded to obtain thin layers. The layers were dried in an oven and placed under vacuum overnight before preparing the coin cell battery CR2032 in Li/CPE/Li configuration. The coin cells were assembled in the glove box. The lithium transference number was measured following Bruce-Vincent-Evans equation at RT (2), where ΔV is 10 mV, I_0 and I_{SS} the initial and steady state currents and R_0 and R_{SS} are the resistances obtained from EIS analysis before and after polarization. The coin cells were tested by dc polarization, applying 10 mV during 7200 s. EIS analysis to determine the ionic conductivity were acquired before and after the chronoamperometry.

$$tLi^+ \frac{I_{SS}(\Delta V - R_0 I_0)}{I_0(\Delta V - R_{SS} I_{SS})} \quad (2)$$

2.2.5. Field-Emission Gun Scanning Electron Microscopy (FEGSEM)

The electrolyte-free samples were analyzed morphologically using FEGSEM Nova NanoSEM 230 working at 5 kV and at 5 mm of distance. The samples were treated previously with ethanol to remove the ionic liquid following the procedure described in the literature [20]. This procedure included changing the solvent twice a day, for one week and drying the samples in a vacuum oven at 70 ºC overnight. Cryofractured samples were analyzed after coating with gold in a gold sputtering (2 nm Au).

2.3. Solid Polymer Electrolyte Preparation

The solid polymer electrolytes were prepared following two different procedures described below, depending whether the samples contain nanoparticles or not. The weight of reagents was calculated for 30 g of total sample according to the wt.% content listed in table 1. Once the samples have been cured they were prepared to adapt the form for each technique samplers.

Table 1. Composition of Hybrid solid polymer electrolytes.

	wt.%					
Sample	**L**	**P**	**ILE**	**Li(1M)**	**PC**	**Al**
L65P35(ILE30)Li	41.82	22.52	30	5.7	-	-
L70P30(ILE40)Li	36.71	15.74	40	7.6	-	-
L65P35(ILE40)Li	34.2	18.3	40	7.6	-	-
L60P40(ILE40)Li	34.47	20.98	40	7.6	-	-
L70P30(ILE45)Li	35.55	13.95	45	8.5	-	-
L65P35(ILE45)Li	30.22	16.27	45	8.5	-	-
L60P40(ILE45)Li	27.9	18.6	45	8.5	-	-
L70P30(ILE50)Li	28.44	12.19	50	9.4	-	-
L65P35(ILE50)Li	26.41	14.22	50	9.4	-	-
L60P40(ILE50)Li	24.38	16.25	50	9.4	-	-
L70P30(ILE40)(PC5)Li	33.21	14.23	40	7.6	5	-
L65P35(ILE40)(PC5)Li	30.84	16.60	40	7.6	5	-
L65P35(ILE30)Li(Al2)	40.52	21.8	30	5.7	-	2
L70P30(ILE40)Li(Al2)	35.31	15.13	40	7.6	-	2
L70P30(ILE45)Li(Al2)	31.15	13.35	40	8.5	-	2
L70P30(ILE50)Li(Al2)	27.04	11.59	40	9.4	-	2

Procedure A (For samples without nanoparticles): In a flat bottom jar the lithium salt was dissolved in the ionic liquid. Then, both resins L and P were weighted in the same jar and the mixture was degassed under vacuum at 80ºC for 15 minutes. Then, the hardeners DDS and XB3473 were added, and the mixture was stirred under vacuum for 10 more minutes. The mixture was placed on a metallic mold and let to cure at 140ºC for 8 hours, as previously described.

 doi:10.20944/preprints202406.1894.v1

Procedure B (for samples containing Al_2O_3 nanoparticles): In a flat bottom jar the lithium salt was dissolved in the ionic liquid. Alumina was added to the previous solution and the nanoparticles were dispersed by ultrasonication in a Hielscher ultrasonic processor UP400 St at 0.5 pulse cycles and 50% amplitude for 1.5 h Then, both resins L and P were weighted in the same jar and the mixture was degassed under vacuum at 80°C for 15 minutes. Then, the hardeners DDS and XB3473 were added, and the mixture was stirred under vacuum for 10 more minutes. The mixture was placed on a metallic mold and let to cure at 140ºC for 8 hours, as previously described.

2.4. Supercapacitor Fabrication

The electrodes of CuO NPs on woven carbon fiber were fabricated following the procedure previously reported in the literature [26]. The Structural supercapacitor was fabricated by Vacuum Assisted Resin Infusion Moulding (VARIM) as reported [24] and using the CPE L70P30(ILE50)Li(Al2). The composite was cured in an oven at 140ºC for 8 hours. The supercapacitors were composed by two layers of WCF electrodes with a two-layer GF separator between them. Copper sheets were also attached to each CFRP electrode by using silver ink to ensure a good electrical contact. EIS test was carried out in the composites in a frequency range of $10x10^6$ -0.1 Hz. The tests were also performed in an AUTO- LAB PGSTAT302N module with a software Nova 2.1.

3. Results and Discussion

3.1. Thermomechanical and morphologycal characterization of the electrolytes

In this study, samples of electrolytes were prepared keeping in mind to enhance the electrochemical and mechanical properties simultaneously. We study the effect of increasing the amount of ionic liquid (40, 45 and 50 wt. % **ILE**) and structural resin content (60, 65 and 70 wt. % of **L** resin). The effect of the addition of propylene carbonate (PC) and ceramic nanoparticles (alumina) was also studied. Table 2 shows the mean values of the storage modulus (E'), loss modulus (E'') and glass transition temperature (T_g), as well as their standard deviations, obtained through the DMTA analysis.

Table 2. Thermomechanical Properties obtained by DMTA analysis.

Entry	Sample	T_g (°C)	E′ (MPa) (T = 30ºC)	E′′ (MPa) (T = 30ºC)
1	L70P30(ILE40)Li	70.7 ± 0.9	1032 ± 41	94 ± 6
2	L65P35(ILE40)Li	57 ± 2	659 ± 27	108 ± 8
3	L60P40(ILE40)Li	55 ± 2	539 ± 87	104 ± 17
4	L70P30(ILE45)Li	69 ± 2	773 ± 127	71 ± 2
5	L65P35(ILE45)Li	56 ± 3	506 ± 93	82 ± 4
6	L60P40(ILE45)Li	44.8 ± 0.5	222 ± 19	72 ± 3
7	L70P30(ILE50)Li	73 ± 1	675 ± 81	61,8 ± 0,9
8	L65P35(ILE50)Li	57 ± 4	530 ± 145	73 ± 14
9	L60P40(ILE50)Li	50 ± 2	328 ± 79	74 ± 12
10	L70P30(ILE40)(PC5)Li	63 ± 2	603 ± 122	76 ± 7
11	L65P35(ILE40)(PC5)Li	50 ± 1	504 ± 26	101 ± 5
12	L70P30(ILE40)Li(Al_2)	72 ± 2	1231 ± 84	112 ± 5
13	L70P30(ILE45)Li(Al_2)	72 ± 2	781 ± 77	74 ± 3
14	L70P30(ILE50)Li(Al_2)	76.6 ± 0.8	696 ± 18	69 ± 1

Concerning the amount of ionic liquid included (40, 45 or 50 wt.%), it was possible to observe better mechanical performance at lower ionic liquid content for all the formulations. The higher values for the storage modulus (E′) were obtained for those samples containing 40% of ILE (from 539 to 1032 MPa at 30°C, entries 1-3). Surprisingly, the T_g values do not varied in this concern, being around 70°C for the samples L70P30 containing 40, 45 and 50 wt% of ILE (entries 1, 4 and 7). The

 doi:10.20944/preprints202406.1894.v1

same behavior was observed for those T_g values of samples L65P35 and L6P40. Concerning the amount of the more structural resin (**L**, from 60 to 70 wt.%), as increases to 70% the T_g and the storage modulus (E') was also found to increase (entries 1-9), as it was expected and observed in previous studies [23]. From a mechanical perspective, the samples containing 70% of **L** resin appear as the most appropriate for structural applications, since as soon as the **L** content is below 70 wt.% the storage modulus drop irremediably. The incorporation of propylene carbonate was then studied in two formulations L70P30(ILE40)Li and L65P35(ILE40)Li (entries 10 and 11) and it was observed a more remarkable drop in the storage modulus for the resin L70P30(ILE40) (from 1032 to 603 MPa) than for the resin with lesser L content (from 659 to 504 MPa). This additive was only added to samples containing 40% of ILE to avoid extreme loss of mechanical performance. The T_g in both cases were lower, decreasing 7ºC. Alumina nanoparticles were added to samples with formula L70P30(ILEX)Li (entries 12-14), to improve and recover mechanical strength. The sample with 40 wt.% ILE (entry 12) exhibits the best improvement with 1,23 GPa of storage modulus. For the other samples (45 and 50 wt.% ILE) the effect was not so remarkable as the values were practically the same as without nanoparticles. The T_g values with the addition of nanoparticles slightly increased in these three cases.

Figure 1 shows the results of storage modulus E' and T_g for all the samples studied. It can be observed that when alumina (2 wt.%) is included in the electrolytes L70P30 for 40, 45 and 50% of ILE, slightly increases the T_g of the samples with different % of ionic liquid regarding the initial values. The best sample performance was found for the sample containing 40% of ILE and alumina, L70P30(ILE40)Li(Al_2) (entry 12).

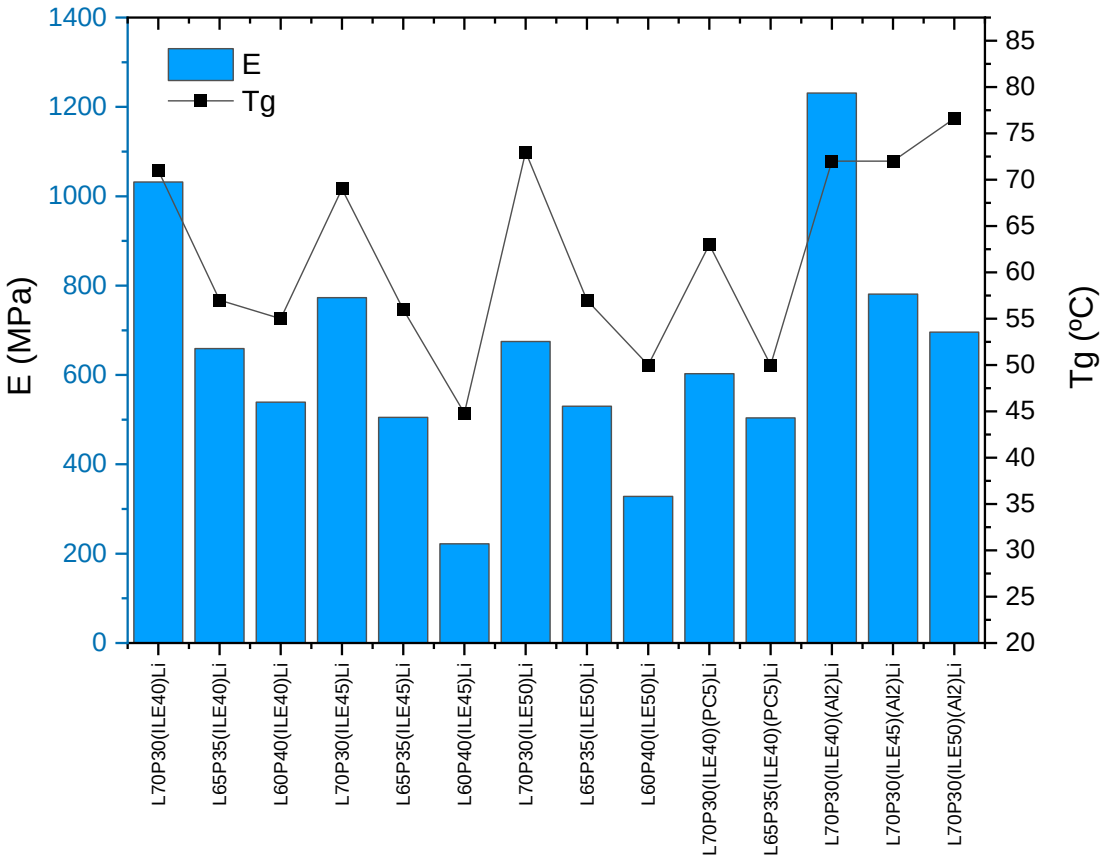

Figure 1. Storage modulus (E', blue bars) and glass transition temperature (T_g, black squares) of the samples.

 doi:10.20944/preprints202406.1894.v1

3.2. Electrochemical characterization of electrolytes

All samples were analyzed by EIS to calculate the ionic conductivity. The values are listed in Table 3.

The ionic conductivities of all the polymer electrolytes prepared in this work are between 7.6×10^{-8} and 5.7×10^{-5} S/cm. In general, as decrease the **L** content in the resin blend the ionic conductivities increased due to the more elastomeric nature of resin **P**, that favor the ionic movements through the bulk. This behavior has been observed in other blends where there are two or more resins with different nature.

The addition of ionic liquid also affects the ionic conductivities, for 40 wt.% the samples exhibit the lowest ionic conductivity values (~$\times 10^{-7}$ S·cm^{-1}, entries 1-3). These values can be improved at least one order of magnitude when a plasticizer as propylene carbonate (PC) is added, reaching up to 1.2×10^{-6} S·cm^{-1} (entry 11). On the contrary, the samples containing 50 wt.% of ionic liquid did not show the best ionic conductivity values, being between 7.2×10^{-7} and 6.1×10^{-6} S·cm^{-1} (entries 7-9). For this samples, an exudated of ionic liquid leak appears after some days meaning poor stability to keep a homogeneous solid.

Table 3. Electrochemical data for the solid electrolytes .

Entry	Sample	σ_0 (S·cm^{-1})	σ_1 (S·cm^{-1})	C_{sp} (μF/cm^2)	Stability range (V)
1	L70P30(ILE40)Li		2.6×10^{-7}	0.30	0.3
2	L65P35(ILE40)Li		2.9×10^{-7}	1.74	0.3
3	L60P40(ILE40)Li		3.5×10^{-7}	3.76	0.8
4	L70P30(ILE45)Li		1.6×10^{-6}	21.22	1.2
5	L65P35(ILE45)Li		1.5×10^{-6}	44.03	1.0
6	L60P40(ILE45)Li		2.6×10^{-6}	109.39	1.7
7	L70P30(ILE50)Li		7.2×10^{-7}	29.64	2.2
8	L65P35(ILE50)Li		8.8×10^{-7}	18.44	1.1
9	L60P40(ILE50)Li		6.1×10^{-6}	67.57	1.8
10	L70P30(ILE40)(PC5)Li		4.8×10^{-7}	7.50	1.4
11	L65P35(ILE40)(PC5)Li		1.2×10^{-6}	30.44	1.2
12	L70P30(ILE40)Li(Al2)	2.0×10^{-5}	3.6×10^{-7}	4.61	2.4
13	L70P30(ILE45)Li(Al2)	2.5×10^{-5}	4.2×10^{-6}	9.11	2.6
14	L70P30(ILE50)Li(Al2)	2.7×10^{-5}	5.7×10^{-6}	2.95	2.3

[1] no lithium.

The introduction of alumina nanoparticles improve the ion mobility in all cases (Figure 2), reducing the ionic liquid leaking process. In the Figure 3, the storage modulus, T_g and ionic conductivities are represented. The only 2 samples that reach the requirements of E' > 1GPa are those containing a 40 wt. % of ionic liquid and 7.6 wt.% of lithium content, then at higher ionic liquid contents the storage modulus drops dramatically. The ionic conductivities of these two samples are in the same order of magnitude of the rest even if they do not exhibit the best values (Figure 2). The combination of the addition of alumina and lithium salt has a small synergistic effect where the T_g and storage modulus were found to increase simultaneously.

Preprints.org (www.preprints.org) | NOT PEER-REVIEWED | Posted: 26 June 2024 doi:10.20944/preprints202406.1894.v1

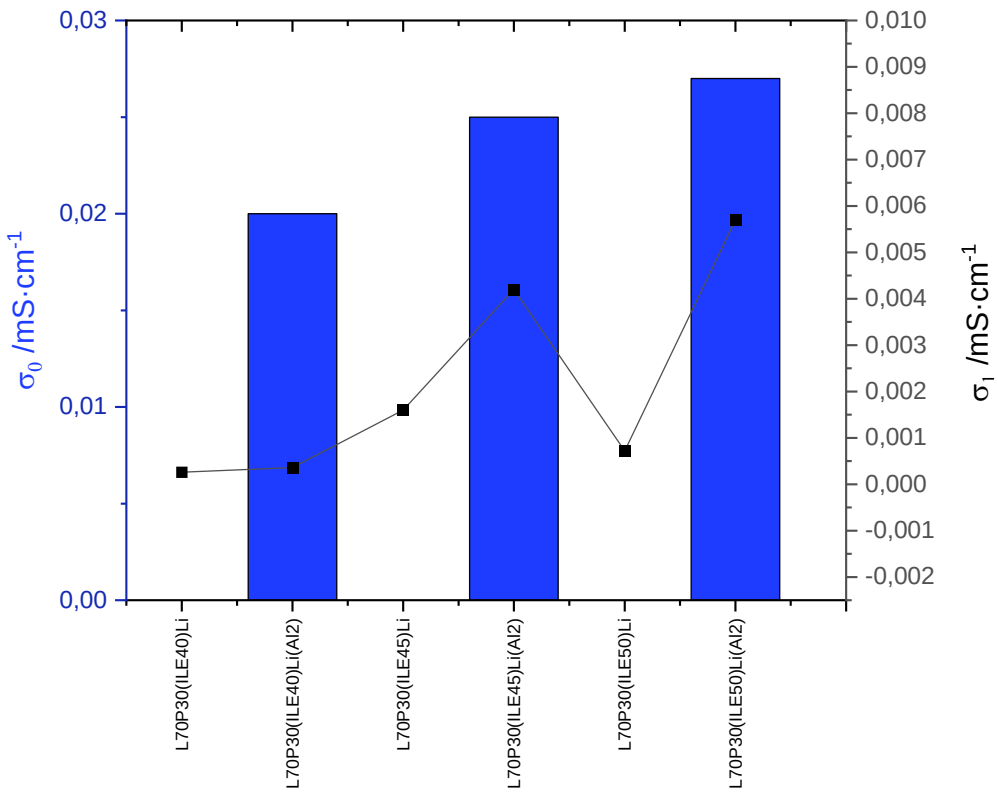

Figure 2. Ionic conductivities of the electrolytes

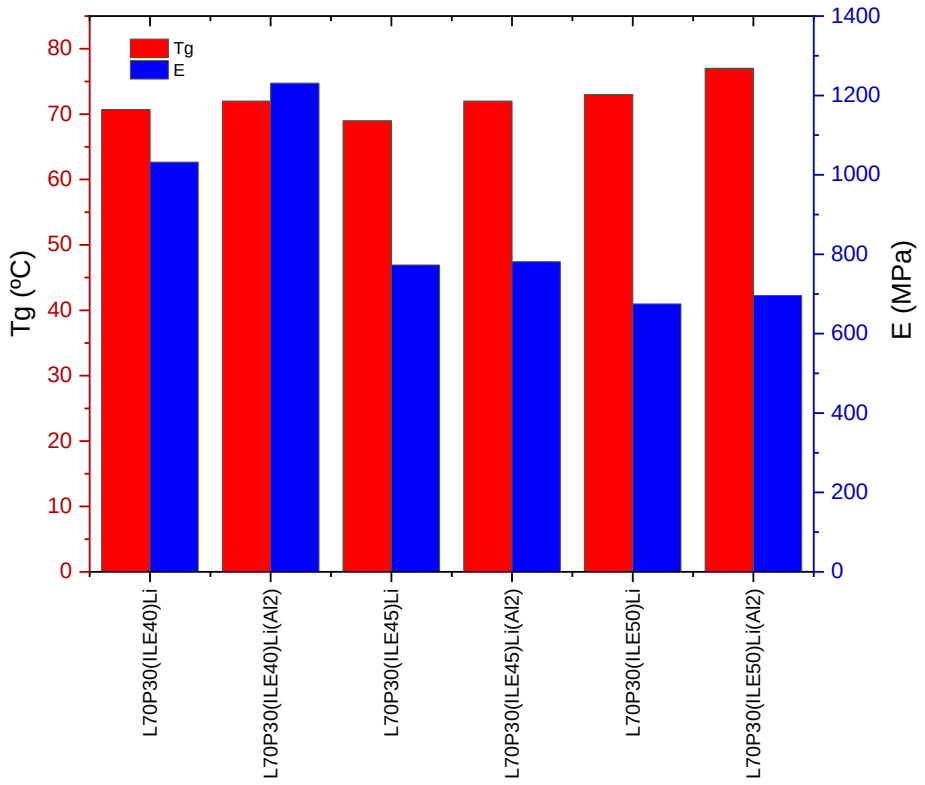

Figure 3. Thermomechanical and electrochemical parameters of the electrolytes

 doi:10.20944/preprints202406.1894.v1

Some samples were analyzed by FEGSEM (Figure 4) to check the difference in the ionic liquid content and the addition of nanoparticles. The SEM images at different magnifications for samples L70P30(ILE40)Li, L70P30(ILE50)Li and L70P30(ILE40)Li, (Figure 4a-c, 4d-f and 4g-i, respectively). The microstructure of the crosslinked resins with different ionic liquid contents (40 and 50 wt.%) showed homogenous solid phases, not presenting a biphasic structure. It is possible observed that when the ionic liquid content increases the microstructure look more irregular with roughness.

The roughness is even higher when alumina nanoparticles are included. The nanoparticles are not well defined at these magnifications (Figure 4g-i), but there is no evidence of big agglomeration or nanoparticle clusters.

In a previous study performed using the same epoxy resin system and ionic liquid, the sample L65P35(ILE30)Al_2 exhibit the best balance between electrochemical and mechanical properties [23]. To compare the effect of the addition of lithium salt and alumina at the same time in this formulation, another set of samples was prepared (Table 4). As it has been previously observed, the addition of lithium can have a positive effect in the stability of the electrolyte [18], and this observation it was reproduce in our system where the storage modulus has increase when lithium was added (table 1, entries 2 and 5 vs table 4, entries 2 and 3). However, in those cases the T_g was slightly lower when lithium was included. The addition of alumina, as it has been previously observed, increased the T_g of the electrolytes being more remarkable for lower ionic liquid content (30 wt.%, table 4 entries 1 and 4). The best ionic conductivity values were obtained for those samples only containing alumina (Table 4, entries 4- 6) compared to samples without lithium and alumina (Table 4, entries 1-3). The simultaneous addition of lithium salt and alumina improve the storage modulus and the ionic conductivity in comparison to the samples modified only with lithium salt (Table 4, entries 7 and 8), but only improve the storage modulus compared to the sample modify only with alumina (Table 4, entries 4 and 8).

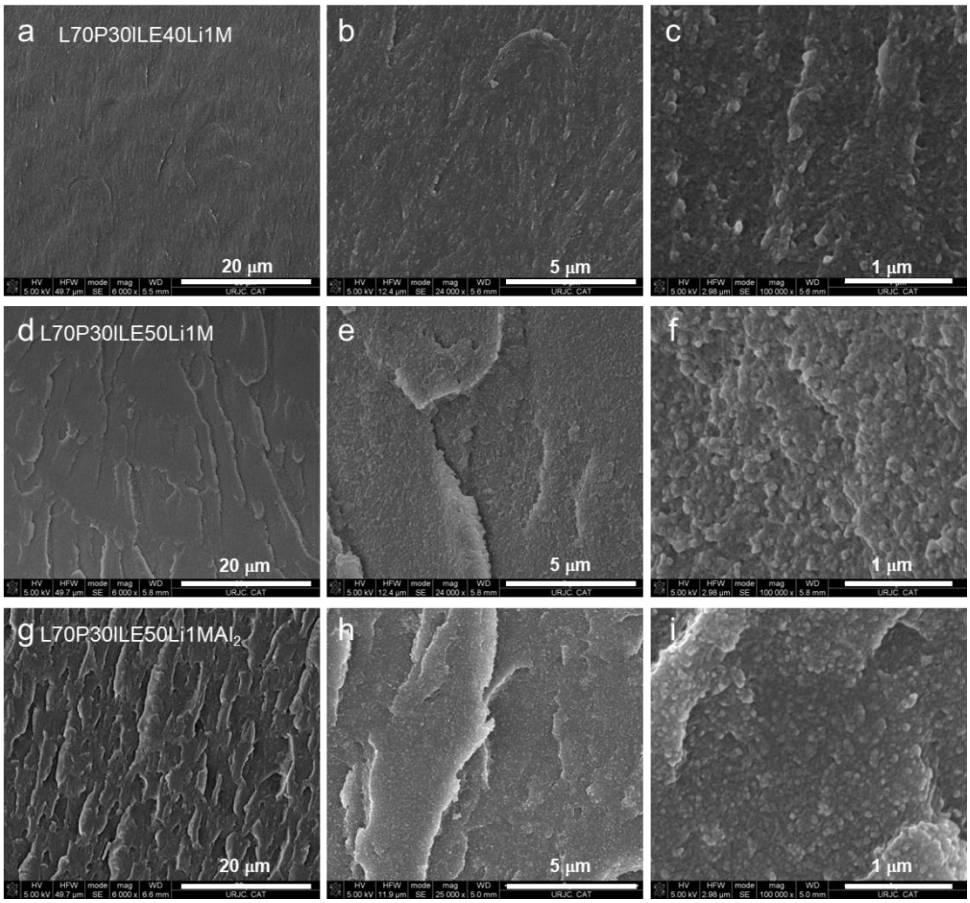

Figure 4. FEGSEM images at different magnifications of the epoxy resins (**a**-**c**) L70P30(ILE40)Li, (**d**-**f**) L70P30(ILE50)Li and (**g**-**i**) L70P30(ILE50)LiAl$_2$.

 doi:10.20944/preprints202406.1894.v1

This detrimental effect on the ionic conductivity by addition of lithium salt has been previously observed [18,27], in some cases, when the lithium concentration in an imidazole-based ionic liquid solution is low (<0.3 M) or high (>1.0 M) [28]. Some authors associate this effect to an increase in viscosity and a reduction in the mobility of ions in the electrolyte [17,28]. Choi and coworkers have found that the lithium salt (LiTFSI) concentration within the electrolyte mixture plays a crucial role in the formation of a bicontinuous nanoscale ion channel confined in the epoxy matrix changing the ionic and epoxy domains. In those cases, the ionic conductivity varied in more than two orders of magnitude range by changing the LiTFSI molar concentration and decreased as increased the Li content [29]. Despite this, the electrolytes fabricated in this study are exceptionally robust, compared with the best epoxy systems found in the literature. The ionic conductivity can be improved by the addition of alumina nanoparticles, and, at the same time, it demonstrates the mechanical stability of the solid.

A comparison of the SPEs/CPEs developed in this work with some of the best representative systems found in the literature are depicted in Figure 5. In the figure, a star indicates the ideal multifunctional electrolyte. The green circle corresponds to system L70P30(ILE40)Li without alumina, which is very robust, but the ionic conductivity is still very low. As soon as alumina nanoparticles are included the ionic conductivity increases to a very competitive level. The best CPE developed using the same resin blend without lithium and reported previously L65P35(ILE30)Al2 (red circle), was very closed to the ideal performance. The idea to reproduce an electrolyte for LIBs with this outstanding electrochemical and mechanical behavior was not possible only by the incorporation of lithium salt, as it can be observed in the Table 4, probably due to lithium atoms can act as plasticizers leading to a more homogeneous mixture (entry 8). However, the ionic conductivity was not so high as expected, they are very promising considering less than 10 % of lithium is contained in the formulation. Moreover, the storage modulus for this sample is very competitive.

Table 4. Electrochemical data for the solid electrolytes .

Entry	Sample	T_g (ºC)	E′ (MPa) (T = 30ºC)	σ_0 (S·cm^{-1})	σ_1 (S·cm^{-1})
1[1,2]	L65P35(ILE30)	65 ± 2	1202 ± 10	-	1.3×10^{-7}
2[1]	L65P35(ILE40)	68 ± 2	495 ± 60	-	1.4×10^{-5}
3[1]	L65P35(ILE45)	63 ± 3	401 ± 80	-	4.5×10^{-5}
4[1,2]	L65P35(ILE30)Al$_2$	83 ± 1	1213 ± 164	7.0×10^{-4}	1.6×10^{-6}
5[1]	L65P35(ILE40)Al$_2$	70 ± 2	461 ± 62	6.8×10^{-5}	9.6×10^{-6}
6[1]	L65P35(ILE45)Al$_2$	65 ± 3	469 ± 89	1.8×10^{-4}	1.8×10^{-7}
7	L65P35(ILE30)Li	68 ± 1	1235 ± 20	-	7.6×10^{-8}
8	L65P35(ILE30)Li(Al$_2$)	85 ± 1	1224 ± 103	1.4×10^{-5}	5.5×10^{-7}

[1]no lithium [2]Ref [23].

To check the effect of temperature on the ionic conductivities in the best systems found in this study L65P35(ILE30)Al2 and L70P30(ILE40)Al2, the samples were heated in an oven, connected to the potentiostat. After the heating the temperature was led to equilibrate for a certain time (30 minutes), the EIS analysis was measured to calculate the ionic conductivity through the resistances.

 doi:10.20944/preprints202406.1894.v1

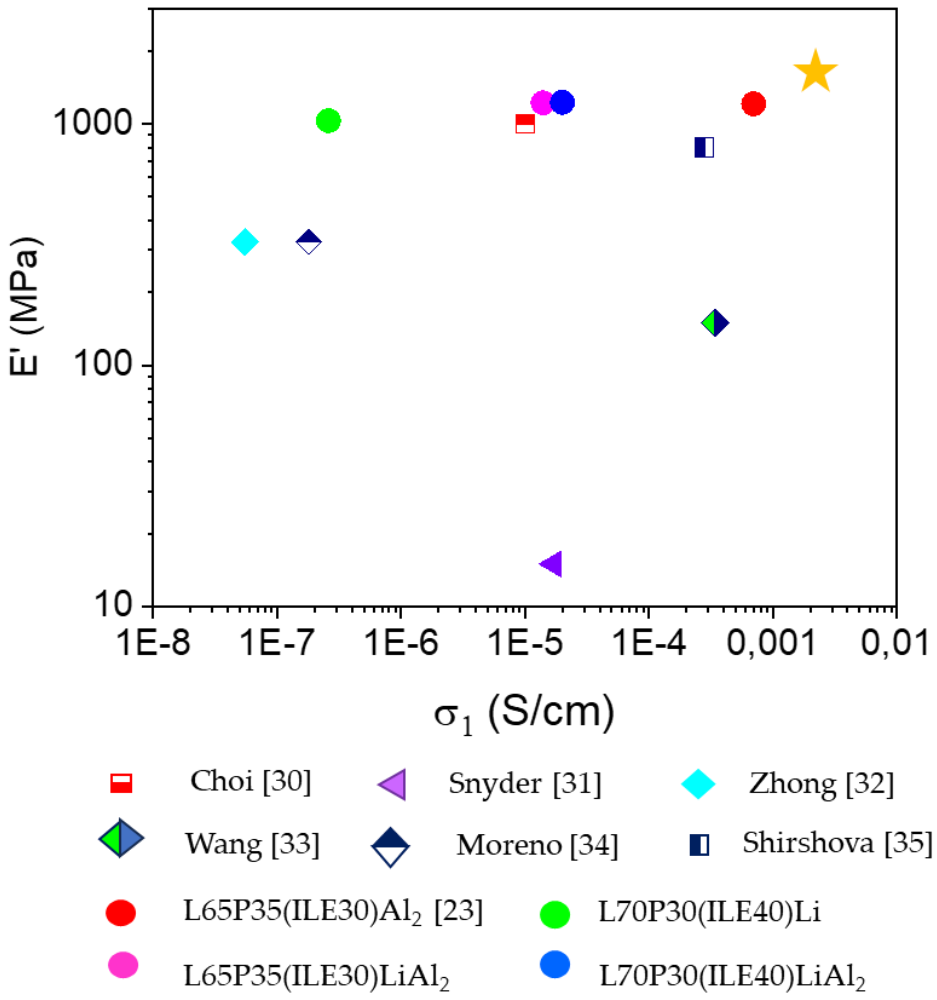

Figure 5. Mechanical and electrochemical comparison of the electrolytes

The Ln of ionic conductivity values (those corresponding to the bulk and grain boundaries) were plot against the inverse of temperature (1000/T(K^{-1}). The plots are shown in Figures 5a and 5b. Both composite electrolytes were fitted to the Arrhenius model and the activation energies were calculated and are shown in Figure 5c. These values obtained agree with the best results obtained for the system L70P30(ILE40)LiAl2. For the sample L65P35(ILE30)LiAl2 the activation energy values are higher being the same for the two conduction mechanisms studied. Regarding the ionic conductivity mechanism, the system L70P30(ILE40)LiAl2 showed two different values of activation energy, where the activated energy associated to the Li salt and ionic liquid immobilized in Alumina NPs was smaller and favored than the ionic conductivity associated to the Li/ions in the bulk. These results can be explained if it is considered that Li salt is dissolved in ionic liquid and this electrolyte is adsorbed or immobilized in the nanoparticles surface (Figure 5d and 5e). In Figure 5e the blue line path is the lithium ionic conduction through the bulk as in SPEs. The ochre line path corresponds to the lithium ionic conduction way by a percolation through the surface of the nanoparticles as it has been previously determined for hybrid electrolytes [36,37]. In this case, as the content of the ionic liquid is higher the ions can move more easily compared to the ions hopping through the bulk.

 doi:10.20944/preprints202406.1894.v1

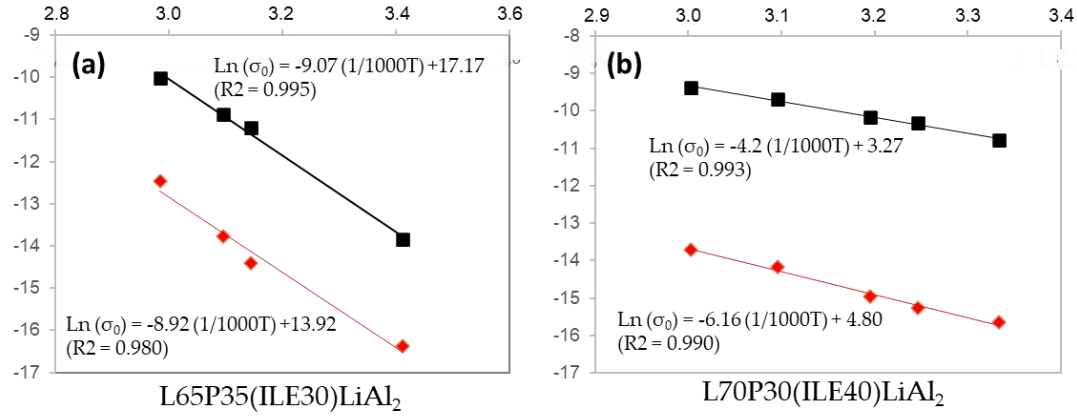

(c)

E_a (eV)	L65P35(ILE30)$LiAl_2$	L70P30(ILE40)$LiAl_2$
Grain boundary	0.78	0.34
Bulk	0.77	0.53

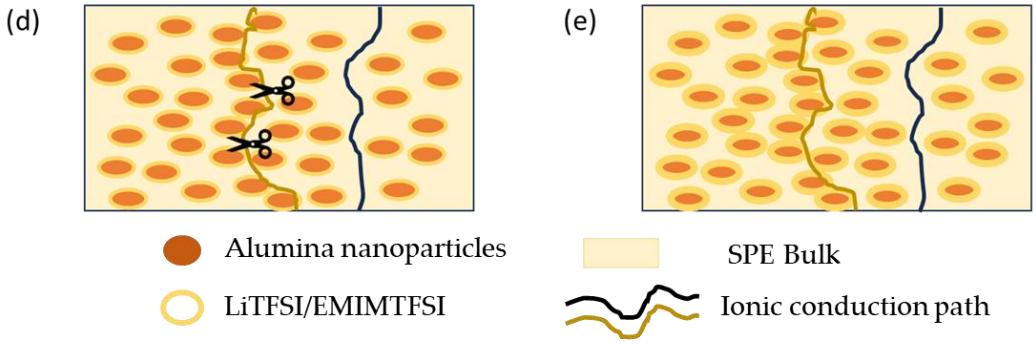

Figure 6. a) Arrhenius type ionic conduction mechanism for L65P35(ILE)30LiAl2 and b) for L70P30(ILE)40LiAl2 Ionic conductivities if the electrolytes, c) Activation energy in eV for the two ionic conductivities, d and e) conduction paths in the CPEs through the bulk (black line) and through the grain boundaries (yellow line).

The lithium transference number of electrolyte L70P30(ILE40)LiAl2 was calculated, and it was found to be t_{Li^+} = 0.13, this number is usually related to the availability of free lithium in the mixture [38]. For systems based on PEO and LiTFSI when the ratio of EO:Li is over 3 the t_{Li^+} decreased dramatically [39]. In our case the EO units (from PEGDGE) give an EO:Li ratio of 14:1, meaning that the whole network is more hindered and there are countless interactions between lithium and its environment (anions, alumina NPs, etc.), that can explain the low value obtained. Nevertheless, the ionic conductivity that can be obtained for this system at 60ºC is 0.085 mS/cm, closer to the optimum value expected for a solid electrolyte.

3.3 Supercapacitors performance of composite polymer electrolytes

To test the applicability of the CSEs, we assembled a symmetric supercapacitor. Figure 7 shows the proof of concept and the results of the EIS test of the device. In the EIS test (Figure 7d, e) it can be observed an incomplete depressed semicircle at high frequencies followed by an irregular spike at low frequencies. This non-perfect semicircle curve corresponds to a parallel resistance-constant phase element. The spike at low frequencies can be fitted to a sum of depressed semicircles with a high resistance. Thus, the inset in Figure 7d show the equivalent circuit and in Figure 7e the data corresponding to the fitting. The device CuO-WCF/WGF/CuO-WCF embedded in the L70P30(ILE40)LiAl2 matrix successfully powered a red LED light but only for a couple of minutes (Figure 7a-c).

Attempts of a structural supercapacitor and battery completely manufactured inside the glove box in a pouch cell are currently in progress.

 doi:10.20944/preprints202406.1894.v1

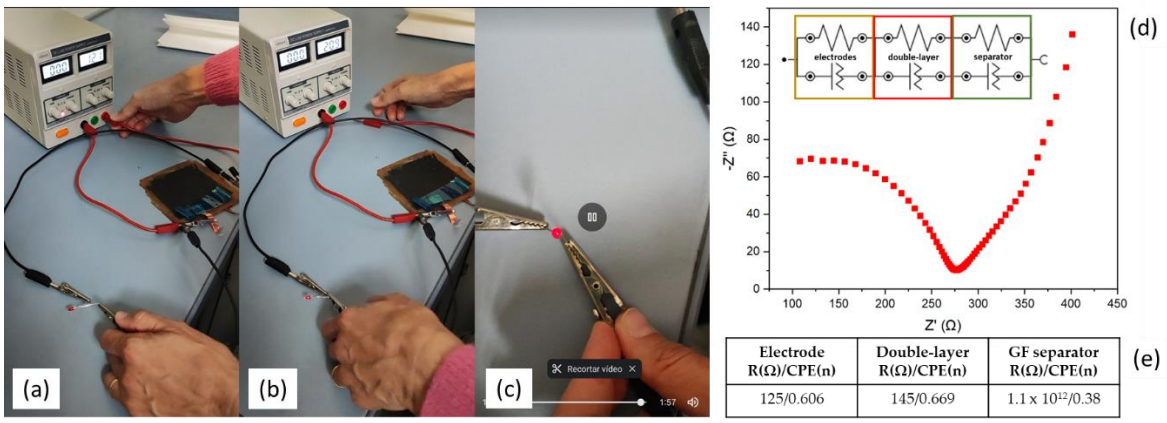

Electrode R(Ω)/CPE(n)	Double-layer R(Ω)/CPE(n)	GF separator R(Ω)/CPE(n)
125/0.606	145/0.669	1.1 x 10^{12}/0.38

Figure 7. a-c) Sequence of LED powered on d) EIS curve and equivalent circuit showed inset e) Activation energy in eV for the two ionic conductivities, d and e) values of the resistance and constant phase element (CPE) of the equivalent circuit

5. Conclusions

New SPEs and CPEs based on epoxy resin blends using 1-ethyl-3-methyl-imidazolium bis(trifluoromethylsulfonyl)imide ionic liquid, lithium bis(trifluoromethylsulfonyl)imide salt and alumina nanoparticles (13 nm) were prepared and the effect of resin composition (60-70 wt.% of structural based on DGEBA) and the ionic liquid content (from 30 to 50 wt.%) were studied. The resin blends containing 40 wt.% of ionic liquid were found to be the optimum without observing any trace of exudated. The mechanical properties were improved increasing the amount of DGEBA based epoxy resin (**L**) in their final composition. Regarding the electrochemical properties, the addition of alumina nanoparticles was found to increase the ionic conductivities, and this effect was attributed to the interfacial alumina-electrolyte interaction in the polymer matrix. We have reach good thermal and mechanical properties for systems L70P30, higher than other similar systems previously reported (T_g > 70 ◦C, E′ >1.2 GPa).

Author Contributions: Bianca K. Muñoz: Investigation, Methodology, Conceptualization, Formal analysis, Visualization, Writing – original draft. Jorge Lozano: Investigation, Methodology, Formal analysis. María Sánchez: Writing – review & editing, Funding acquisition. Alejandro Ureña: Writing – review & editing, Funding acquisition. All authors have read and agreed to the published version of the manuscript.

Funding: This work was supported by the Agencia Estatal de Investigación of Spanish Government [Project MULTISENS PID2022-136636OB-I00].

Institutional Review Board Statement: Not applicable.

Data Availability Statement: No new data were created.

Conflicts of Interest: The authors declare no conflicts of interest.

References

1. Wazeer, A.; Das, A.; Abeykoon, C.; Sinha, A.; Karmakar, A. Composites for electric vehicles and automotive sector: A review. G*reen Energy and Intelligent Transportation*, **2023**, *2*, 100043.
2. Cheah, L. Cars on a Diet: The material and energy impacts of passenger vehicle weight reduction in the US. PhD thesis, Massashussets Institute of Technology , USA, **2010**. Available: https://dspace.mit.edu/handle/1721.1/62760.
3. Jin, T.; Singer, G.; Liang K.; Yang, Y. Structural batteries: Advances, challenges and perspectives. *Materials Today*, **2023**, *62*, 151-167.
4. Greenhalgh, E.S.; Nguyen, S.; Valkova, M.; Shirshova, N.; Shaffer, M.S.P.; Kucernak, A.R.J. A critical review of structural supercapacitors and outlook on future research challenges. *Composites Science and Technology*, **2023**, *235*, 109968.

 doi:10.20944/preprints202406.1894.v1

5. Klongkan, S. ; Pumchusak, J. Effects of nano alumina and plasticizers on morphology, ionic conductivity, thermal and mechanical properties of PEO-LiCF3SO3 solid polymer electrolyte. *Electrochim. Acta* **2015**, *161*, 171–176.
6. Lin, C.; Hung, C.; Venkateswarlu, M; Hwang, B. Influence of TiO2 nano-particles on the transport properties of composite polymer electrolyte for lithium-ion batteries. *J. Power Sources* **2005**, *146* (1–2), 397–401.
7. Jiang, G.; Maeda, S.; Yang, H.; Saito, Y.; Tanase, S.; Sakai, T. All solid-state lithiumpolymer battery using poly (urethane acrylate)/nano-SiO2 composite electrolytes, *J. Power Sources* **2005**, *141* (1) 143–148.
8. Feng, Q.; Yang, J.; Yu, Y.; Tian, F.; Zhang, B.; Feng, M.; Wang, S. The ionic conductivity, mechanical performance and morphology of two-phase structural electrolytes based on polyethylene glycol, epoxy resin and nano-silica. *Mater. Sci. Eng. B Solid-State Mater. Adv. Technol.*, **2017**, *219*, 37-44.
9. Zhang, Y.; Zhao, Y.; Gosselink, D.; Chen, P. Synthesis of poly (ethylene-oxide)/nanoclay solid polymer electrolyte for all solid-state lithium/sulfur battery, *Ionics* **2015**, *21*, 381–385.
10. Chand, N.; Rai, N.; Agrawal, S.L.; Patel, S.K. Morphology, thermal, electrical and electrochemical stability of nano aluminium-oxide-filled polyvinyl alcohol composite gel electrolyte, *Bull. Mater. Sci*. **2011**, *34*, 1297–1304.
11. Song, Z.; Liu, X.; Ding, J.; Liu, J.; Han, X.; Deng,Y.; Zhong, C.; Hu, W. Poly(Acrylic Acid)-Based Nanocomposite Gel Polymer Electrolyte with High Mechanical Strength and Ionic Conductivity Towards Long-Cycle-Life Flexible Zinc–Air Battery, **2022**, (Available at SSRN. 4109010).
12. Kwon, S.J.; Jung, B.M.; Kim, T.; Byun, J.; Lee, J.; Lee, S.B.; Choi, U.H. Influence of Al2O3 nanowires on ion transport in nanocomposite solid polymer electrolytes. *Macromolecules* **2018**, *51*, 10194–10201.
13. Wang, J.; Fan, L.; Du, Q.; Jiao, K. Lithium ion transport in solid polymer electrolyte filled with alumina nanoparticles, *Energy Adv*. **2022**, *1*, 269.
14. Croce, F.; Persi, L.; Scrosati, B.; Serraino-Fiory, F.; Plichta, E.; Hendrickson, M. A. Role of the Ceramic Fillers in Enhancing the Transport Properties of Composite Polymer Electrolytes. *Electrochim. Acta* **2001**, *46* (16), 2457−2461.
15. Dissanayake, M. A. K. L.; Jayathilaka, P. A. R. D.; Bokalawala, R. S. P.; Albinsson, I.; Mellander, B.-E. Effect of Concentration and Grain Size of Alumina Filler on the Ionic Conductivity Enhancement of the (PEO)9LiCF3SO3:Al2O3 Composite Polymer Electrolyte. *J. Power Sources* **2003**, *119*−*121*, 409−414.
16. Chandra, A.N.; Sungmook, L.; Guk-Hwan,L.; Wonoh, L. Epoxy-based multifunctional solid polymer electrolytes for structural batteries and supercapacitors. a short review. *Frontiers in Chemistry*, **2024**, *12*, 1330655.
17. Shirshova, N.; Bismarck, A.; Greenhalgh, E. S.; Johansson, P.; Kalinka, G.; Marczewski, M. J.; Shaffer, M. S. P.; Wienrich, M. Composition as a Means To Control Morphology and Properties of Epoxy Based Dual-Phase Structural Electrolytes. *J. Phys. Chem. C* **2014**, *118* (49), 28377−28387.
18. Muñoz, B. K.; del Bosque, A.; Sánchez, M.; Utrilla, V.; Prolongo, S. G.; Prolongo, M. G.; Ureña, A. Epoxy Resin Systems Modified with Ionic Liquids and Ceramic Nanoparticles as Structural Composites for Multifunctional Applications. *Polymer*, **2021**, *214*, 123233.
19. Wendong, Q.; Dent, J.; Arrighi, V.; Cavalcanti, L.; Shaffer, M. S. P.; Shirshova, N. Biphasic Epoxy-Ionic Liquid Structural Electrolytes: Minimising Feature Size through Cure Cycle and Multifunctional Block-Copolymer Addition. *Multifunct. Mater*. **2021**, *4* (3), 035003.
20. Shirshova, N.; Bismarck, A.; Carreyette, S.; Fontana, Q.P.V.; Greenhalgh, E.S.; Jacobsson, P.; Johansson, P.; Marczewski, M.J.; Kalinka, G.; Kucernak, A.R.J.; Scheers, J.; Shaffer, M.S.P.; Steinke, J.H.G.; Wienrich, M. Structural supercapacitor electrolytes based on bicontinuous ionic liquid–epoxy resin systems *J. Mater. Chem. A.*, **2013**, *1*, 15300-15309.
21. Tu, V.; Asp, L.E.; Shirshova, N.; Larsson, F.; Runesson, K.; Jänicke, R. Performance of bicontinuous structural electrolytes. *Multifunct. Mater.*, **2020**, *3*, 025001.
22. Choi, U.H., Jung, B.M. Ion Conduction, Dielectric and Mechanical Properties of Epoxy-Based Solid Polymer Electrolytes Containing Succinonitrile. *Macromol. Res.* **2018**, *26*, 459–465.
23. Del Bosque,A.; Muñoz, B.K.; Sánchez, M. Ureña, A. Thermomechanically Robust Ceramic/Polymer Nanocomposites Modified with Ionic Liquid for Hybrid Polymer Electrolyte Applications *ACS Applied Energy Materials* **2022,** *5* (4), 4247-4258.

 doi:10.20944/preprints202406.1894.v1

24. Sánchez-Romate, X.F. ; Del Bosque, A.; Artigas-Arnaudas, J.; Muñoz, B.K.; Sánchez, M.; A. Ureña. A proof of concept of a structural supercapacitor made of graphene coated woven carbon fibers: EIS study and mechanical performance. *Electrochim. Acta*, **2021**, *370* , 137746.
25. Tianwei Jin, Gerald Singer, Keyue Liang, Yuan Yang, Structural batteries: Advances, challenges and perspectives, *Materials Today*, **2023**, *62*, 151-167.
26. Muñoz, B.K.; González-Banciella, A.; Ureña, D.; Sánchez, M.; Ureña, A. Electrochemical Comparison of 2D-Flexible Solid-State Supercapacitors Based on a Matrix of PVA/H3PO4. *Polymers* **2023**, *15*, 4036.
27. S. Seki, Y. Ohno, Y. Kobayashi, H. Miyashiro, A. Usami, Y. Mita, H. Tokuda, M. Watanabe, K. Hayamizu, S. Tsuzuki, M. Hattori, N. Terada, Imidazolium-based room-temperature ionic liquid for lithium secondary batteries, *J. Electrochem. Soc.* **2007**, *154*, A173–A177.
28. Z.P. Rosol, N.J. German, S.M. Gross, Solubility, ionic conductivity and viscosity of lithium salts in room temperature ionic liquids, *Green Chem*. **2009**, *11*, 1453–1457.
29. Y.H. Song, T. Kim, U.H. Choi, Tuning morphology and properties of epoxy-based solid-state polymer electrolytes by molecular interaction for flexible all-solid-state supercapacitors, *Chem. Mater.* **2020**, *32*, 3879–3892.
30. U.H. Choi, B.M. Jung. Ion conduction, dielectric and mechanical properties of epoxy-based solid polymer electrolytes containing succinonitrile *Macromol. Res.*, **2018**, *26*, 459-465.
31. J.F. Snyder, R.H. Carter, E.D. Wetzel Electrochemical and mechanical behavior in mechanically robust solid polymer electrolytes for use in multifunctional structural batteries. *Chem. Mater.*, **2007**, *19*, 3793-3801.
32. J. Ji, B. Li, W.-H. Zhong. Simultaneously enhancing ionic conductivity and mechanical properties of solid polymer electrolytes via a copolymer multi-functional filler. *Electrochim. Acta*, **2010**, *55*, 9075-9082.
33. Y.J. Wang, D. Kim. Crystallinity, morphology, mechanical properties and conductivity study of in situ formed PVdF/LiClO4/TiO2 nanocomposite polymer electrolytes. *Electrochim. Acta*, **2007**, *52*, 3181-3189.
34. M. Moreno, R. Quijada, M.A. Santa Ana, E. Benavente, P. Gomez-Romero, G. González. Electrical and mechanical properties of poly(ethylene oxide)/intercalated clay polymer electrolyte. *Electrochim. Acta*, **2011**, *58*, 112-118.
35. Q. Wendong, J. Dent, V. Arrighi, L. Cavalcanti, M.S.P. Shaffer, N. Shirshova Biphasic epoxy-ionic liquid structural electrolytes : minimising feature size through cure cycle and multifunctional block-copolymer addition *Multifunct. Mater.*, **2021**, *4*, 035003.
36. W. Zaman,N. Hortance,M. B. Dixit,V. De Andrade,K. B. Hatzell, *J. Mater. Chem. A* **2019**, *7*, 23914–23921.
37. Tan, SJ., Zeng, XX., Ma, Q. et al. Recent Advancements in Polymer-Based Composite Electrolytes for Rechargeable Lithium Batteries. *Electrochem. Energ. Rev*. **2018**, *1*, 113–138.
38. Mengyang Jia, Muhammad Khurram Tufail, Xiangxin Guo. Insight into the Key Factors in High Li+ Transference Number Composite Electrolytes for Solid Lithium Batteries. *ChemSusChem* **2023**, *16*, e2022018.
39. K. Pożyczka, M. Marzantowicz, J.R. Dygas, F. Krok, Ionic conductivity and lithium transference number of poly(ethylene oxide):litfsi system, *Electrochimica Acta*, **2017**, *227*, 127-135